Microporous and Mesoporous Materials 230 (2016) 30–38

Contents lists available at ScienceDirect

Microporous and Mesoporous Materials

journal homepage: www.elsevier.com/locate/micromeso

On the drastic reduction of organic structure directing agent in the steam-assisted crystallization of zeolite with hierarchical porosity

Mita Rilyanti [a], Rino R. Mukti [a, b, *], Grandprix T.M. Kadja [a], Masaru Ogura [c], Hadi Nur [d], Eng-Poh Ng [e], Ismunandar [a]

[a] Division of Inorganic and Physical Chemistry, Faculty of Mathematics and Natural Sciences (FMIPA), Institut Teknologi Bandung, Jl. Ganesha 10, Bandung, 40132, Indonesia
[b] Research Center for Nanosciences and Nanotechnology, Institut Teknologi Bandung, Jl. Ganesha 10, Bandung, 40132, Indonesia
[c] Institute of Industrial Science, The University of Tokyo, 4-6-1 Komaba, Meguro-ku, Tokyo, 153-8505, Japan
[d] Center for Sustainable Nanomaterials, Ibnu Sina Institute for Scientific and Industrial Research, Universiti Teknologi Malaysia, 81310 UTM Skudai, Johor, Malaysia
[e] School of Chemical Sciences, Universiti Sains Malaysia, 11800 USM, Penang, Malaysia

ARTICLE INFO

Article history:
Received 24 February 2015
Received in revised form
13 April 2016
Accepted 28 April 2016
Available online 29 April 2016

Keywords:
ZSM-5
Hierarchical
SAC
OSDA

ABSTRACT

The absence of organic structure directing agent (OSDA) in the synthesis of zeolite has shown progress recently, nevertheless the formation mechanism is still not clearly understood and the technique cannot be fully generalized for the synthesis of various types of zeolite frameworks. In this research, the drastic reduction of OSDA in the synthesis of ZSM-5 employing the steam-assisted crystallization (SAC) was studied. The used tetrapropylammonium bromide as OSDA in the synthesis of ZSM-5 was one-fifth and one-twentieth of typical amount reported in literature. Upon OSDA reduction, the crystallization leads to the formation of ZSM-5 with hierarchical pore structure revealed by SEM and TEM images in which it is different compared to the parent spherical-like crystal morphology of ZSM-5 synthesized without reducing the OSDA amounts. A quantitative analysis of the X-ray diffractograms suggests that 100% crystallinity could not be achieved in the sample synthesized under the OSDA reduction confirming that the orientation of crystal growth is not similar to the conventional coffin-type ZSM-5 crystal. The deviancy in crystal growth is further associated with the formation of mesopores originated from severe defect planes of ZSM-5. On the verge of gradual disappearance, a broadened distribution of mesoporosity could return the crystallinity to 100% in which faulty elongated crystal shape, close to typical coffin-type growth orientation appeared as the product after commencing the Oswald ripening of longer period of synthesis time. The conventional hydrothermal synthesis may not be used for crystallizing ZSM-5 when the OSDA was one-twentieth of typical starting amount making the SAC to be an appropriate technique for synthesizing ZSM-5 under drastically reduced OSDA, in particular to simultaneously perform the hierarchically porous zeolite.

1. Introduction

Zeolites are widely used as ion exchangers, sorbents, and catalysts in petrochemical and fine chemical industries [1–5]. These days, zeolites continue to find potential uses in emerging areas for commercial applications such as membrane [6–8], the field of photonics [9] and medical support [10]. ZSM-5 (MFI-type) has been one of the zeolites most in demand due to its potential use as an industrial fluid catalytic cracking (FCC) catalyst for enhancing selectivity towards propylene [11]. The synthesis pathway of ZSM-5 can be economically efficient or inefficient, depending on the required specification of the ZSM-5 product for certain applications [12]. For example, low acidity ZSM-5 (high Si/Al ratio) has to be synthesized by using additional structure-directing agent (OSDA) in an extensive amount, but the highly acidic ZSM-5 (low Si/Al ratio) can be synthesized in low OSDA amounts or even in the absence of OSDA [13–15]. The organic tetrapropyl ammonium ion

* Corresponding author. Division of Inorganic and Physical Chemistry and Research Center for Nanosciences and Nanotechnology, Institut Teknologi Bandung, Jl. Ganesha 10, Bandung, 40132, Indonesia.
E-mail address: rino@chem.itb.ac.id (R.R. Mukti).

http://dx.doi.org/10.1016/j.micromeso.2016.04.038
1387-1811/

(TPA^+) has been commonly used as OSDA for synthesizing ZSM-5 and the rational use of either high or low OSDA amounts is in line with the amount of inorganic cations compensating the negatively charged zeolite framework at the elementary step of zeolite formation [16]. A synergistic amount of organic and inorganic cation can be also useful for synthesizing a cation-rich framework. Interestingly, the presence of only inorganic cation (OSDA-free) in the aluminosilicate gel system has been reported to successfully realize the formation of ZSM-5 [17–20]. However, the mechanism of OSDA-free route is not clearly understood and this may involve zeolite itself as a seed in place of OSDA during the synthesis of high silica zeolites [21–24].

In addition to hydrothermally crystallize the zeolite gel under conventional technique, ZSM-5 gel containing TPA^+ can also be hydrothermally treated under steam-assisted crystallization (SAC) as part of the dry-gel conversion (DGC) technique [25–27]. Wang et al. reported that by using this technique the resulting zeolite may show hierarchical porosity [28–30]. Hierarchical zeolites with additional mesoporosity (2–50 nm) have been offered as a solution to intracrystalline diffusion limitation of catalyzed reactions [31,32]. The sole presence of micropores (<2 nm) in zeolite may not have been well utilized whenever there is a mass-transfer constraint leading to a poor catalyst performance [33]. In principle, the objective of creating mesoporosity on a zeolite crystal surface is to enhance molecular diffusivity, the overall rate of catalyzed processes due to ease of pore access and to inhibit the catalyst deactivation process. One of the direct methods to synthesize mesoporous zeolite applies simultaneously the OSDA and mesopore-generating molecule (mesoporogen) [34–36]. The advantages of using this mesoporogen are the ability to tune the mesopore size and to establish the mesostructures [37,38]. However, there are disadvantages of applying this complex route, such as high consumption of energy to thermally remove both of the organic compounds for pore-opening, complicated nucleation and considerably high cost for industrial commercialization. To this solution, we would like to apply SAC for converting the conventional gel of ZSM-5 containing typical TPA^+ ion into hierarchically porous ZSM-5. The low templated or complete absence of OSDA in the syntheses of zeolites is receiving great interest nowadays, although there is a lack of understanding [39–42]. In current research, we have conducted a study on systematic reduction of OSDA amounts in the synthesis of ZSM-5. The used TPA^+ was one-fifth to one-twentieth of typical amount commonly found in literature [29]. The effect of these minimum amounts of TPA^+ ions in the conventional gel of ZSM-5 was correlated to the crystal morphology, crystallization kinetics, generation of inter-crystalline mesoporosity, aluminosilicate composition and influence of the dry-gel condition prior to the hydrothermal treatment. The optimized condition can be offered as eco-synthesis of hierarchically porous zeolites via a bottom-up procedure. From a practical point of view, the technique using less OSDA is economically beneficial, involves less energy consumption and is probably suitable for large scale production.

2. Experimental

2.1. Gel preparation

The typical gel of ZSM-5 was prepared using a molar composition: 1 SiO_2: x Al_2O_3: 0.14 NaOH: y TPABr: 37.5 H_2O. The values x and y were varied according to the desired Si/Al ratio and amounts of OSDA reduction, respectively. The Si/Al ratios of ZSM-5 samples investigated in this study were 20 and 100. The unreduced OSDA in gel of ZSM-5 applies the TPA^+/Si ratio of 0.24 and this ratio was also reported by Wang et al. showing for the first time that single OSDA can also be used to generate mesoporosity in ZSM-5 [29]. The reduced OSDA followed the TPA^+/Si ratio of 0.05 and 0.012 that are one-fifth and one-twentieth of 0.24 mol of TPA^+, respectively. In the typical preparation of zeolite, a solution was prepared by mixing sodium aluminate ($NaAlO_2$, Sigma-Aldrich), sodium hydroxide (NaOH 50%wt, Merck), tetrapropylammonium bromide (TPABr, Merck) and distilled water. Another solution was prepared by dispersing colloidal silica (LUDOX HS-40, Aldrich) in water. The two solutions were mixed with vigorous stirring at RT for 3 h in a closed bottle. Subsequently, the solution was stirred at RT in an open air and the gel stability was monitored in the first 24 h. After stirring for seven days, the aluminosilicate gel was obtained and further dried in an oven at 100 °C. Series of experiments investigating the effect of temperature during drying process were also conducted.

2.2. Zeolite crystallization

The dry gel conversion (DGC) is a common terminology for crystallizing zeolite precursors in the form of gel under water vapor. The DGC method is further classified into vapor-phase transport (VPT) method and steam-assisted crystallization (SAC) method. The former describes crystallization of dried gel under water vapor in the presence of volatile OSDA such as ethylenediamine whereas the latter describes crystallization of dried gel under water vapor containing a non-volatile OSDA such as tetrapropylammonium hydroxide. The SAC was used in the present experiment and the design of Teflon-lined stainless steel apparatus can be seen in Fig. 1. 0.3 g of gel was transferred into a 10 mL Teflon cup that was positioned inside the larger Teflon liner. 3 g of water was added outside of the cup and the Teflon liner was placed into a 50 mL stainless steel autoclave and heated at 150 °C for several days (up to five days). After finishing the reaction, the autoclave was cooled down to RT and the resulting solid product was filtered, washed and dried. OSDA removal was performed by calcining the sample at 550 °C in air for 6 h at a heating rate of 1 °C/min. The conventional hydrothermal treatment for synthesizing ZSM-5 with various Si/Al ratios under reduced and unreduced OSDA was also carried out for comparative purposes. The applied chemical composition, temperature and synthesis time were identical to the synthesis via SAC.

2.3. Characterization

Powder X-Ray Diffraction (XRD) patterns were recorded on a Bruker D8 diffractometer with Cu Kα radiation to reveal the zeolite topology of the synthesized samples. The crystallinity of the resulting ZSM-5 phase was quantified by taking value of the integrated area from the XRD peak 2θ of 23.05°. This integrated value has been proven to show consistency in explaining the crystallinity in course of crystallization time, whereas other 2θ values show great inconsistency. The percentage of crystallinities were calculated according to equation (1).

$$\%\ \text{Crystallinity} = \left[\frac{\text{Area(sample)}}{\text{Area(reference)}}\right] \text{x} 100\% \quad (1)$$

The crystallinity of all synthesized ZSM-5 is relative to conventional ZSM-5 possessing perfect coffin-type crystals as revealed by scanning electron microscopy (SEM). ZSM-5 for reference was synthesized via conventional hydrothermal treatment using original recipe found in Ref. [29]. All XRD patterns were measured under identical scanning program in the same diffractometer. The systematic collection of data can be useful for the quantitative analysis.

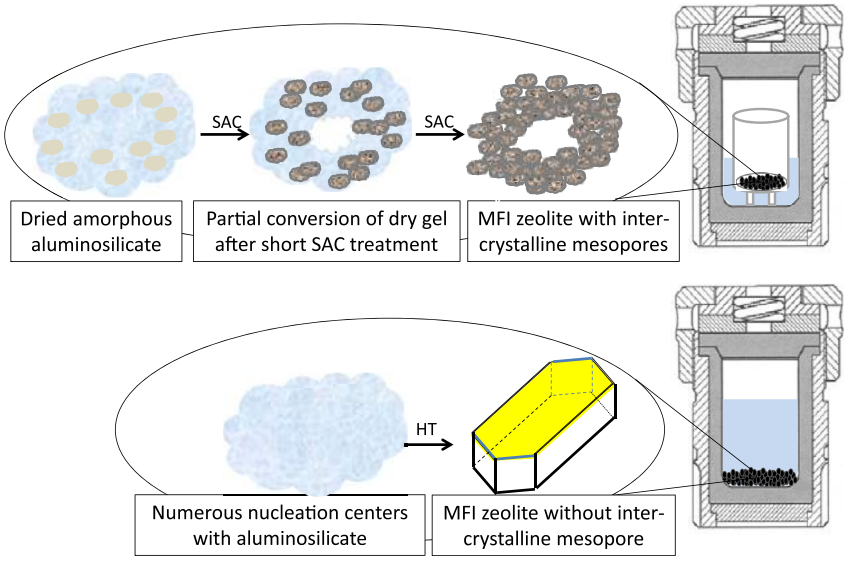

Fig. 1. Illustration of MFI zeolite formation resulted from the steam-assisted crystallization (SAC) and conventional crystallization method via hydrothermal treatment (HT). The conventional crystallization method resulted in coffintype without possessing a hierarchical porosity whereas SAC method resulted in distorted coffintype (up to spherical-like) zeolite morphology possessing a hierarchical porosity with mesopores at inter-crystalline system.

SEM micrographs for all samples were measured on a JEOL-JSM-6510LV microscope. Transmission electron microscope (TEM) was measured using JEOL. Nitrogen adsorption-desorption isotherms were measured using a Quantachrome Autosorb iQ-MP instrument at 77 K whereas Argon adsorption-desorption isotherms were measured at 87 K. Prior to analysis, samples were preheated to 300 °C for 6 h in a vacuum. The specific surface areas (S_{BET}) were calculated using the Branauer-Emmet-Teller (BET) method. The micropore volumes (S_{micro}) and external surface area (S_{ext}) were determined from t-plots (Figs. S1 and S2). The non-local density functional theory (NLDFT), applied to the adsorption branch of the Ar isotherm, was employed to determine both micro- and mesopores size distributions. Solid-state magic-angle spinning nuclear magnetic resonance (MAS NMR) spectra were recorded using single pulse experiment on an Agilent DD2 500 MHz. The ^{29}Si, ^{27}Al and ^{13}C spectra were recorded at resonance frequencies of 99.32, 130.28 and 125.72 MHz with spinning rate of 9 kHz, a pulse width of 1.0 μs and a recycle delay of 5 s. The ^{29}Si and ^{27}Al MAS NMR spectra were reported relative to tetrakis (trimethylsilyl)silane (TTMSS) and $Al(NO_3)_3$, respectively. The NMR spectra were deconvoluted by using a Gaussian function. The integrated areas of the deconvoluted peak were used to quantify the Si/Al framework ratio using the following formula (equation (2)):

$$\left(\frac{Si}{Al}\right) = \sum_{n=0}^{4} I_{Si(nAl)} \Big/ \sum_{n=0}^{4} \frac{n}{4}\left[I_{Si(nAl)}\right] \quad (2)$$

where $I_{Si(nAl)}$ = the total area of Si(nAl).

3. Results and discussion

3.1. OSDA reduction in ZSM-5 synthesis

Steam-assisted crystallization of the typical gel of ZSM-5 in the presence of reduced OSDA amounts was successfully achieved. However, the limitation of synthesis parameter is present. We conducted a series of experiments under reduced OSDA condition comparing the traditional hydrothermal (HT) and steam-assisted crystallization (SAC). Fig. 2 summarizes the successful results of synthesizing ZSM-5 showing only the methods that works well. It can be seen that the reduction of TPA^+ ion from 0.05 to 0.012 has been a good example for discriminating the synthesis method between HT and SAC towards successful ZSM-5 synthesis. When the TPA^+ ion is one-twentieth of the starting amount, it is learned that the SAC is a selective technique for crystallizing ZSM-5. Under this drastic reduction of OSDA, HT is further considered to be unselective method for the ZSM-5 synthesis using either Si/Al ratio of 20 or 100.

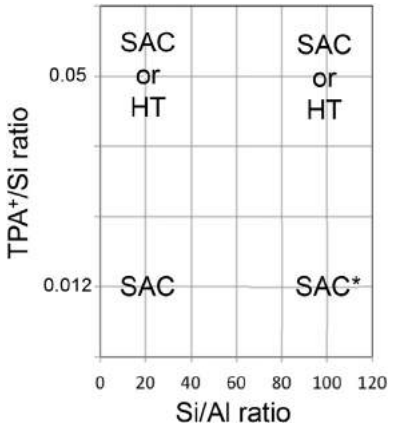

Fig. 2. A chart summarizes the successful results of synthesizing ZSM-5 in present study under reduced OSDA by implementing the HT or SAC method and several synthesis parameters. Asterisk indicates that the resulted ZSM-5 contains MOR zeolite as an impurity.

Fig. 3 shows XRD pattern of ZSM-5 synthesized in the minimum amount of TPA^+ ion. It was observed that the zeolite crystallized faster in the sample containing one-fifth TPA^+ ions than in the sample containing one-twentieth TPA^+ ions. In the presence of one-fifth TPA^+ ions, ZSM-5 showed high crystallinity after 24 h of synthesis time whereas under one-twentieth, ZSM-5 was just crystallized after 48 h. This indicates that the amount of TPA^+ ions plays a significant role as a structure-directing agent to direct the formation of ZSM-5. The crystal morphology appears to be

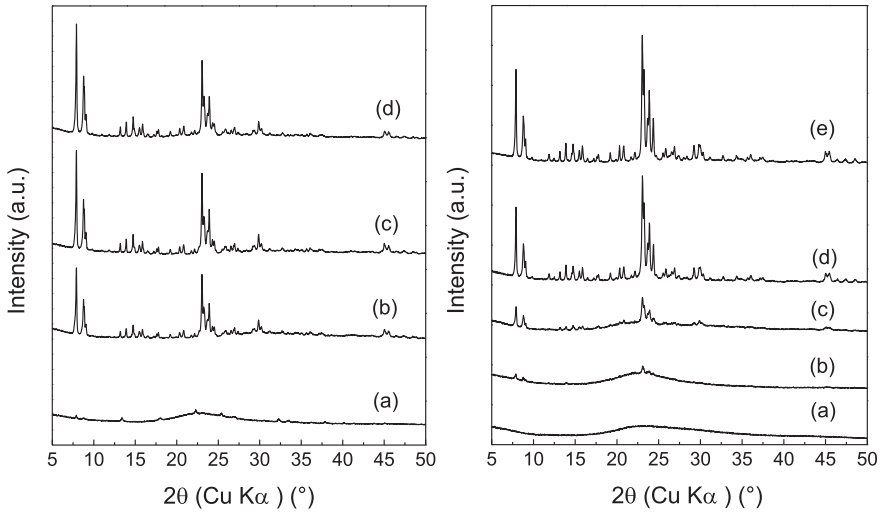

Fig. 3. XRD pattern of ZSM-5 synthesized via SAC method at 150 °C. The TPA^+ was 1/5th (left) of the starting amount and the resulting solid was monitored after synthesizing for (a) 0 h in the dry gel state, (b) 24 h, (c) 48 h and (d) 120 h. The TPA^+ was 1/20th (right) of the starting amount and the resulting solid was monitored after synthesizing for (a) 0 h in the dry gel state, (b) 7 h, (c) 24 h, (d) 48 h and (e) 72 h.

significantly different when comparing ZSM-5 synthesized by reduced TPA^+ ions and unreduced TPA^+ ions (Fig. 4). The typical coffin-like morphology of ZSM-5 was not observed when the unreduced OSDA was used in the steam-assisted crystallization of

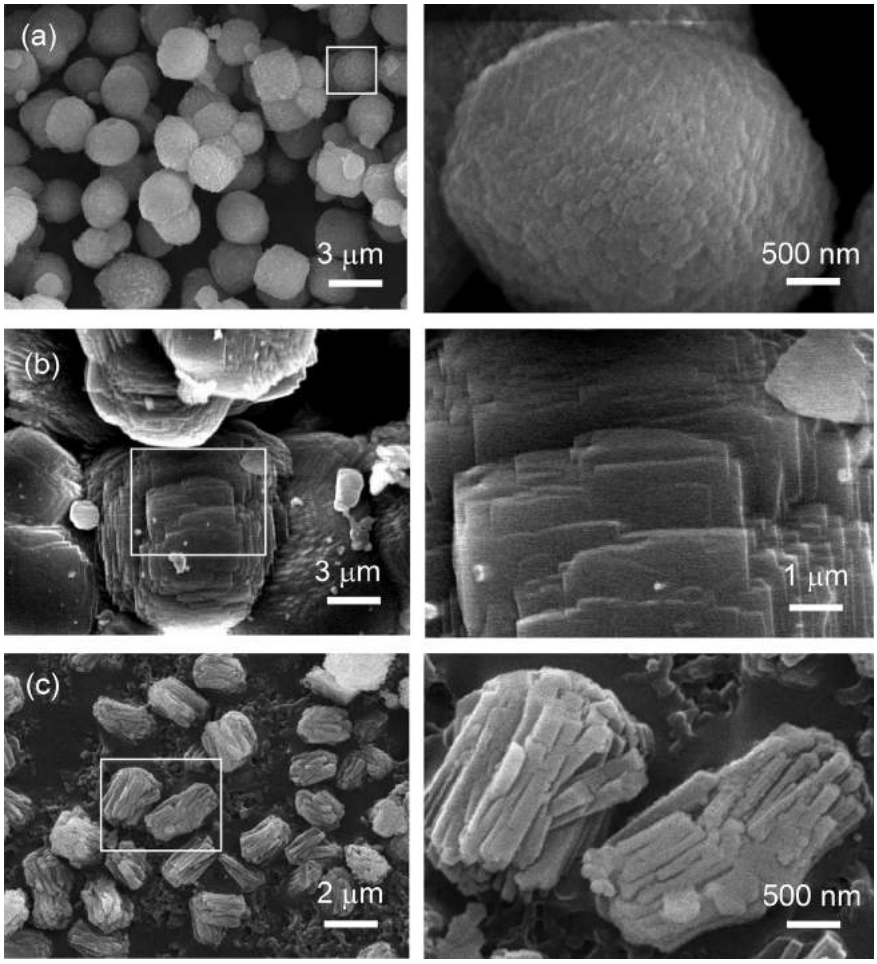

Fig. 4. SEM images of ZSM-5 synthesized via SAC method by employing (a) TPA^+ with starting amount as well as SEM images of ZSM-5 in which the TPA^+ was (b) 1/5th and (c) 1/20th of the starting amount. All images on the right are magnified from its corresponding left image. The synthesis conditions are 150 °C for (a) 120, (b) 120 and (c) 72 h, respectively.

ZSM-5. The resulting ZSM-5 shows a spherical-like morphology, instead. Furthermore, the crystal morphology obtained from applying a low TPA^+ ion amount also different from the unreduced TPA^+ ions on ZSM-5 samples. SEM images reveal a rugged crystal surface, suggesting that the crystallization under these low TPA^+ ion amounts leads to a severe defect planes. We have reproduced this synthesis of ZSM-5 under reduced TPA^+ and still observed similar crystal morphology (Fig. S3).

The ability to reduce the concentration of TPA^+ ions in the synthesis of ZSM-5 might lead to the possibility that ZSM-5 can be obtained in the absence of OSDA. This is due to the fact that synthesis of ZSM-5 in the absence of OSDA can be realized using conventional hydrothermal treatment. Concerning this phenomenon, the first question to address in this study is whether the reduced amount of TPA^+ ions remains intact in the framework during ZSM-5 synthesis, and the second question would be whether the undertaking precursors in the respective molar composition might give ZSM-5 in the absence of TPA^+ ions. The assignment of resonances from the solid-state ^{13}C MAS NMR spectra of as-synthesized zeolite revealed that TPA^+ ion was identified although the concentration had been drastically reduced (Fig. 5). The solid-sate data is supported by the measurement of dissolved TPABr using solution-state ^{13}C NMR confirming that all resonances are identical (Fig. 5a). This may be understood that TPA^+ ion is still intact, residing within the pores of ZSM-5.

The solid-state ^{29}Si MAS NMR spectra show unresolved peaks associated with $Si(OSi)_x\ (O^-)_{4-x}$ where x is the number of -OSi available in the Si environment (Fig. 6). In the case of ZSM-5, the number of −OSi depends on isomorphous substitution of Si with Al as a heteroatom. The isomorphous substitution of Si with Al in zeolite was confirmed by ^{27}Al MAS NMR spectroscopy, revealing that all ZSM-5 showed tetrahedral coordination of Al with a chemical shift at 57 ppm. This ultimately suggests that all Al was substituted in the framework. The ^{29}Si NMR spectra were deconvoluted in order to assign the bands and also to quantify the Si/Al framework ratio. The deconvoluted peaks were assigned as Q_x (*y* Al) or $Si(OT)_x\ (O^-)_{4-x}$, where *x* and *y* is number of adjacent -OT (-OSi or -OAl) and number of -OAl units, respectively. They were identified as Q_4 (0 Al) at −100 and −104.4 ppm, and Q_4 (1Al) at at −96.5 ppm. Moreover, it was clearly shown that spectra depicting ZSM-5 with an Si/Al ratio of 20 and 100 could be easily distinguished from the spectral broadening. ZSM-5 with an Si/Al ratio of 20 tended to give a broader band whereas a narrower band was shown for the Si/Al ratio of 100. The quantitative analysis using Equation (2) and taking the integral area of deconvoluted peaks was in agreement with the spectral observation. The broader band and the narrower band gave final Si/Al ratio of 21 and 73, respectively. These numbers are relatively close to the starting Si/Al ratios. In addition, we have also calculated Si/Al ratio from the X-ray Fluorescence (XRF) analysis and the results give exactly similar Si/Al ratio of 21 and 73 for sample with 1/20th and 1/5th OSDA of starting amount, respectively. This confirms that the presence of unreacted amorphous phase can be neglected.

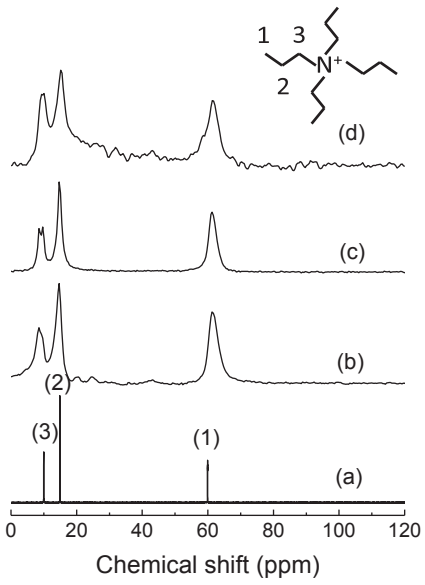

Fig. 5. ^{13}C MAS NMR spectra of TPA^+ in (a) solution and (b–d) solid state ^{13}C MAS NMR of TPA^+ molecule in ZSM-5 synthesized at 150 °C for 24 h by (b) employing the TPA^+ with starting amount and (c, d) TPA^+ with reduced amounts. The TPA^+ was (c) 1/5th and (d) 1/20th of the starting amount.

3.2. Effect of solvent evaporation temperature on crystallization of ZSM-5

The most important factor for synthesizing certain structure of zeolite is gel composition but additional physical treatment to this gel such as heating and stirring, may also affect the synthesis to a significant extent. The evaporation of ZSM-5 conventional gel is the key to accelerating the crystallization of ZSM-5, as well as to turn the solely micropore-type into hierarchically meso/micropore-type properties under reduced OSDA. Fig. 7 show the crystallinity of the resulting solids after the series of gels were treated at various evaporation temperatures prior to the SAC. The crystallization of ZSM-5 can be enhanced by increasing the evaporation temperature of OSDA-reduced gel from 50 to 100 °C. To strongly realize this thermal effect, an experiment of evaporating gel at room temperature was carried out and the results show that ZSM-5 was not crystallized.

On the basis of these facts, the solvent evaporation at an elevated temperature seems to stimulate the formation of nucleation centers. The presence of nuclei certainly allows the crystallization of zeolite, and on the other hand, the absence of nuclei prevents this crystallization. In the case of the SAC method where crystallization is carried out in a somewhat controlled or slow manner, we emphasize that the initial thermal treatment of gel is needed. It is observed from SEM images that the ZSM-5 crystal resulting from solvent evaporated at 100 °C is larger than that from solvent evaporated at 50 °C (Fig. 8). The peak width of the XRD pattern when comparing the two samples further supports the discrepancy in crystal size. In addition to that, the crystal morphology also shows a dramatic difference. In principle, the number of nuclei influences the size of crystals and in this case, the solvent evaporation at 50 °C gives a larger number of nuclei; therefore resulting in smaller crystals of ZSM-5. We believe that there are two reasons for suggesting that the thermal-induced nuclei formation during gel preparation is required to optimize the results of synthesized zeolite, in particular to simultaneously create mesoporosity. The first reason is that less OSDA is contained in the zeolite solution, and the second reason might be the need for a more organized gel matrix by complete removal of all water in the gel prior to the crystallization.

3.3. Hierarchy on the OSDA-reduced ZSM-5

Hierarchically porous zeolites have been attracting considerable attention recently due to demand for a catalyst that is effective in accommodating bulky reactants and solving the diffusion limitation. The synthesis strategy to realize this material normally involves additional yet expensive and non-commercially available compounds, for example unique surfactants to direct the

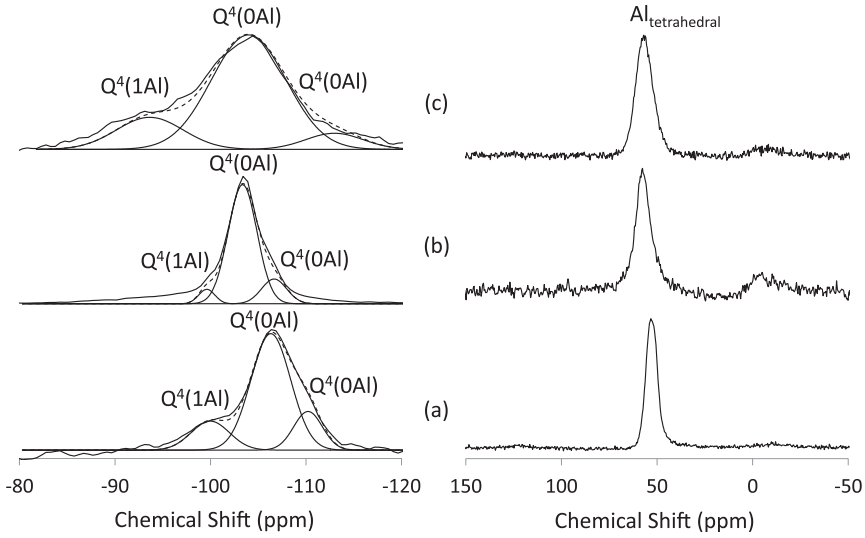

Fig. 6. Solid state ^{29}Si MAS NMR (left) and ^{27}Al MAS NMR (right) of ZSM-5 synthesized at 150 °C for 24 h by (a) employing TPA^+ with starting amount and (b, c) TPA^+ with reduced amounts. The TPA^+ was (b) 1/5th and (c) 1/20th of the starting amount.

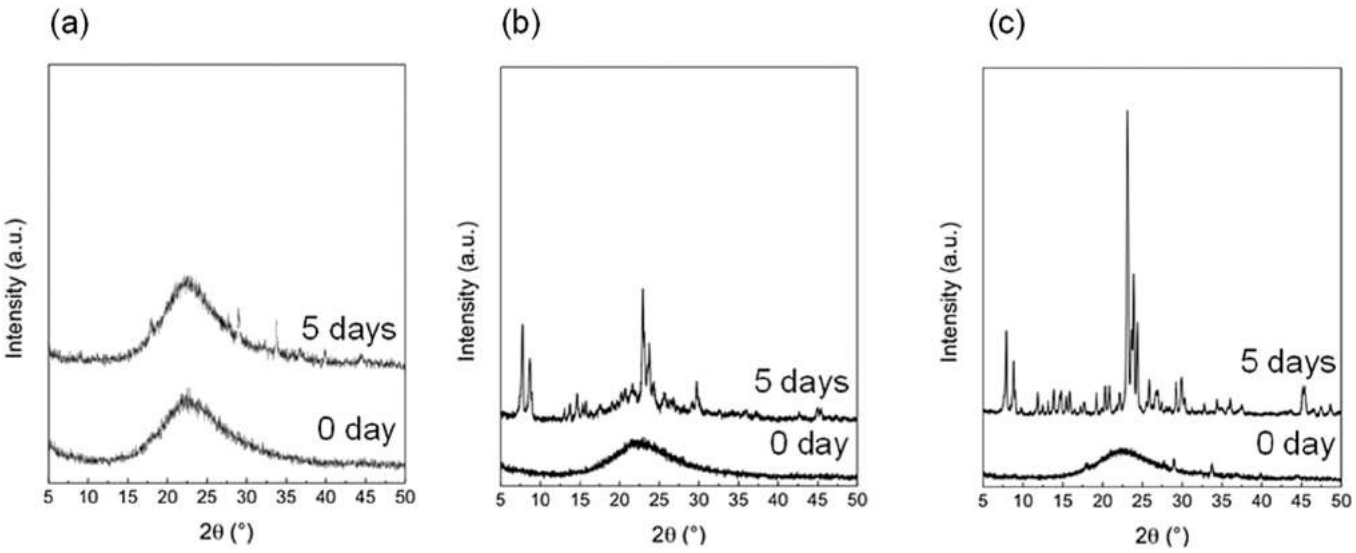

Fig. 7. XRD pattern of ZSM-5 synthesized by employing solvent evaporation of gel precursor at (a) RT, (b) 50 °C and (c) 100 °C in which the TPA^+ was 1/5th of the starting amount.

mesoporosity via micelle formation. In current strategy, we would like to reduce the number of compounds and advantageously to rationally use expensive precursors such as organic SDA. Following the unusual crystal morphology obtained from the OSDA-reduced ZSM-5, we observe that the generation of mesoporosity occurred during the synthesis of ZSM-5 with the reduction of TPA^+ ions to one-fifth (Fig. 9 and Table 1) and one-twentieth (Fig. 10 and Table 2). To investigate the hierarchy of zeolite pore, we observed each condition during the course of crystallization. Prior to zeolite formation, the initial dried gel shows reversible nitrogen adsorption-desorption isotherms of type II, corresponding to a non-porous or possibly macroporous characteristics. After the crystallization of zeolite, this isotherm turns into type IV with a hysteresis loop that is associated with capillary condensation taking place in mesoporosity. The external surface area for the formation of hierarchical ZSM-5 reaches 50 m^2/g. TEM visualized distinct distribution of mesopore for ZSM-5 synthesized by using one-fifth TPA^+. Under one-twentieth TPA^+, the TEM analysis shows large crystal with observed lattice fringes showing the well-defined micropore structure of ZSM-5 (Fig. 11). This observation is also supported with the low external surface area, ca. 6 m^2/g or around 2.4% of the specific surface area, possessed by ZSM-5 synthesized under one-twentieth TPA^+. These morphological changes as a function of TPA^+ using SAC method were reproducible showing the significance of these findings. It has been previously proposed that the scaffolding function of TPA^+ ion may direct both micro- and mesopore formation in which no additional supramolecular template is needed [30]. Therefore, the minimum number of precursors can be realized to perform the zeolite synthesis in one pot. Moreover, in our current research, the TPA^+ ion was successfully reduced, adding the perspective towards less precursors in zeolite synthesis.

In addition to the use of N_2 as probe molecule within the sorption isotherm, Ar sorption experiment may give an accurate value to identify the presence of mesopores in the hierarchical zeolite [43–45]. In some of our samples show steps at P/Po around ~0.2 which are due to the fluid-to-crystalline phase transition of

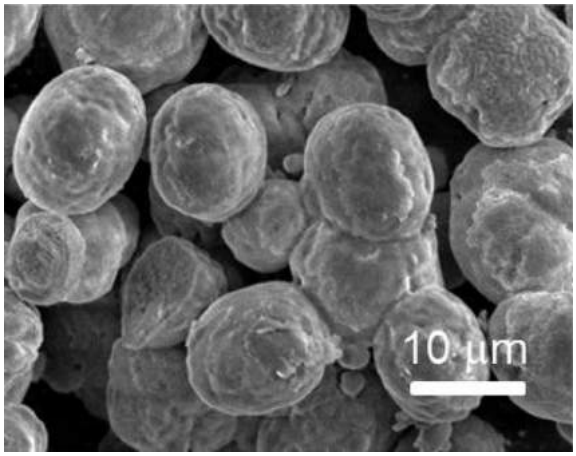

Fig. 8. SEM image of ZSM-5 synthesized via SAC at 150 °C for 120 h by employing solvent evaporation of gel precursor at 50 °C in which the TPA^+ was 1/5th of the starting amount.

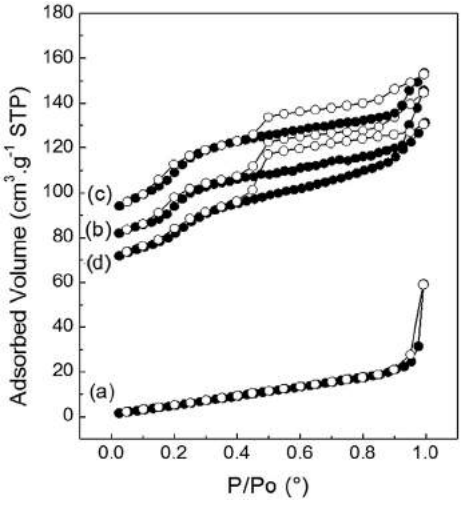

Fig. 9. Nitrogen adsorption-desorption isotherm of ZSM-5. The TPA^+ was 1/5th of the starting amount. The resulting solid was monitored after synthesizing for (a) 0 h, (b) 24 h, (c) 48 h and (d) 120 h.

adsorbed N_2. This will lead to an assignment of artefact as narrow mesopores that is commonly occurred in the interpretation of the N_2 sorption isotherm. A careful attention should be made in analyzing t-plots for these isotherms because of the steps at P/Po around ~0.2. Hence, the relative pressure points should be tagged from the linear regime for the regression of t-plots, as shown in Figs. S1 and S2. In addition to the use of N_2 as probe molecule within the sorption isotherm, Ar sorption experiment may give an accurate value to identify the presence of mesopores in the

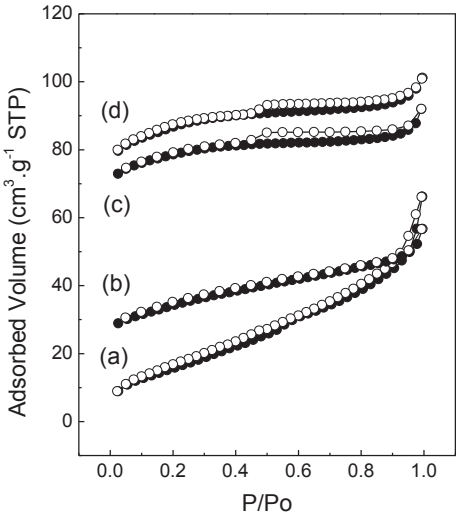

Fig. 10. Nitrogen adsorption-desorption isotherm of ZSM-5. The TPA^+ was 1/20th of the starting amount. The resulting solid was monitored after synthesizing for (a) 0 h, (b) 24 h, (c) 48 h and (d) 72 h.

hierarchical zeolite [43–45]. Unlike N_2, Ar interacts weaker with the zeolite framework resulting in lower extra steps (P/Po = ~10^{-3}) than that of N_2 (P/Po around ~0.2). The use of Ar enables sorption isotherm to be highly useful in assessing materials with pore sizes of narrow mesopores or borderline between micro- and mesopores [46]. Ar sorption isotherms of ZSM-5 synthesized ZSM-5 under one-fifth TPA^+ shows high resolution Ar uptakes at low relative pressure which are related to their adsorption properties in micropores, indicating the preservation of zeolitic microporous framework structure (Fig. S4a). The micropore size distributions derived from the Ar adsorption-desorption isotherms using the NLDFT pore size model evidently confirms the unique ZSM-5 micropore size (around ca. 0.55 nm) (Fig. S4b). In addition, the mesopores size distribution shows the presence of mesopores for ZSM-5 synthesized under one-fifth TPA^+ (Fig. S4c).

Unlike ZSM-5 synthesized under one-fifth OSDA reduction, drastically reducing the OSDA to one-twentieth resulted in ZSM-5 with less mesoporosity in the course of crystallization (Table 2). The external surface area generated from the starting dried gel showed only 6 m^2/g even after zeolite was fully crystallized at 72 h (Table 2). In this situation, the low amount of TPA^+ ion is believed to merely function as zeolite OSDA, thus, further emphasizing that the scaffolding effect of TPA^+ ion is not much in function. In this context, Coppens and co-workers discussed in detail the role of TPAOH in the formation disordered mesopores of a controlled size by means of advanced characterizations such as TEM, DLS, ATR-IR and NMR spectroscopy [47]. They coined TPA^+ ion as non-templating structure-directing in which this organic species can direct the formation of nanoporous material even in the absence of micelles. One of key parameters of the nontemplating structure-

Table 1
Sorption properties of ZSM-5 synthesized by employing solvent evaporation of gel precursor at 100 °C in which the TPA^+ was 1/5th of the starting amount.

Synthesis time (h)	Surface area		Pore volume		
	S_{BET} (m^2/g)	S_{ext}[a] (m^2/g)	V_{total} (cm^3/g)	V_{micro}[a] (cm^3/g)	V_{meso} (cm^3/g)
0	29	29	0.09	0	0.09
24	322	35	0.22	0.15	0.07
48	366	30	0.23	0.17	0.06
120	277	50	0.2	0.12	0.08

[a] Determined using t-plot method.

Table 2
Sorption properties of ZSM-5 synthesized by employing solvent evaporation of gel precursor at 100 °C in which the TPA^+ was 1/20th of the starting amount.

Synthesis time (h)	Surface area		Pore volume		
	S_{BET} (m^2/g)	S_{ext}[a] (m^2/g)	V_{total} (cm^3/g)	V_{micro}[a] (cm^3/g)	V_{meso} (cm^3/g)
0	61	61	0.1	0	0.1
24	103	20	0.05	0.04	0.05
48	223	10	0.14	0.11	0.04
72	247	6	0.16	0.14	0.02

[a] Determined using t-plot method.

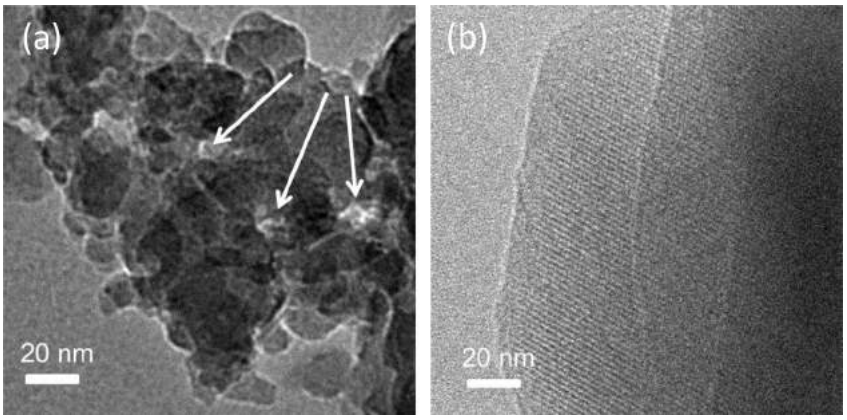

Fig. 11. TEM image of ZSM-5 synthesized by employing solvent evaporated of gel precursor at 100 °C in which the TPA^+ was (a) 1/5th and (b) 1/20th of the starting amount. Arrows showing the presence of mesoporosity.

directing mechanism are identified to have certain TPAOH/TEOS ratio. The drastically low TPA^+ ion in current study may not meet this criterion, therefore high mesoporosity cannot be obtained.

3.4. Crystallinity profile of the OSDA-reduced ZSM-5

The crystallization behavior of ZSM-5 under reduced OSDA can be conclusively described as follows. The crystallization of ZSM-5 was studied by following the kinetics of zeolite formation. A quantitative analysis of the XRD results suggests that the formation of ZSM-5 under one-fifth OSDA over conducted reaction time is equilibrated at 80% crystallinity (Fig. 12). The crystallinity analysis is based on the consideration that a highly crystalline XRD pattern of perfect coffin-type crystals of ZSM-5 possesses 100% crystallinity. This unusual crystallization profile of ZSM-5 synthesized under one-fifth OSDA supports the presence of unlevelled terraces on the crystal surface. The crystal growth experiences severe defect planes allowing the generation of mesoporosity. Unlike ZSM-5 with one-

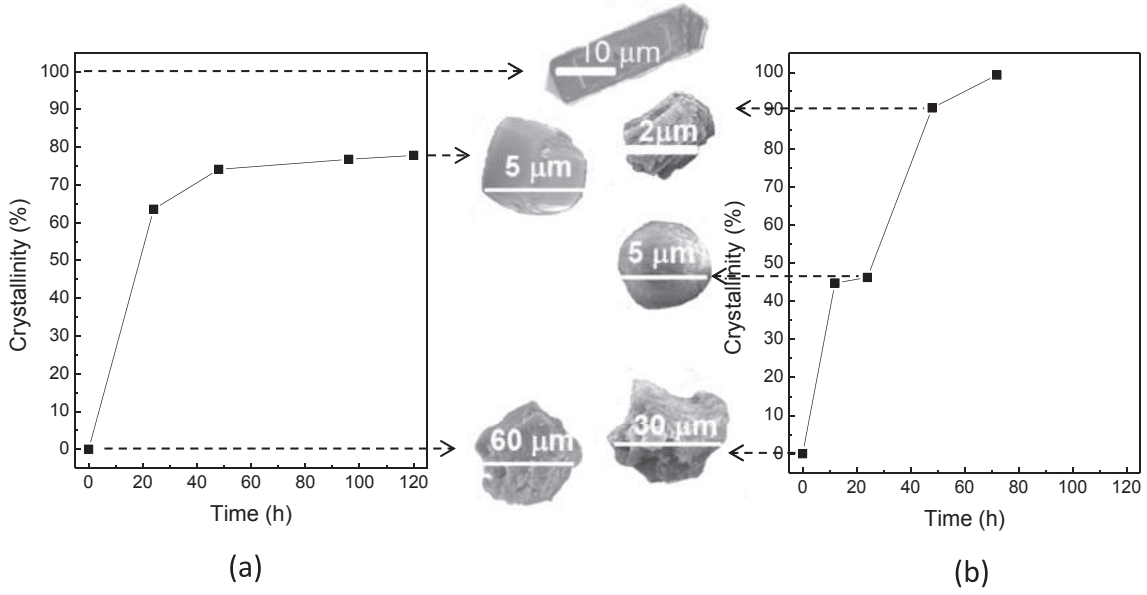

Fig. 12. Crystallinity profile of zeolite synthesized under reduced TPA^+: (a) 1/5th and (b) 1/20th of the starting amount. The crystallinity of 100% refers to the XRD pattern of coffin-type ZSM-5 synthesized using conventional crystallization method.

fifth OSDA, ZSM-5 synthesized under one-twentieth OSDA achieves 100% crystallinity after a slight longer period of time. However, the remaining irregular crystal morphology further supports the hypothesis that the reduction of OSDA clearly distracts the crystallization of ZSM-5.

4. Conclusion

ZSM-5 was successfully crystallized under drastically reduced OSDA amounts when using steam-assisted crystallization (SAC). This modified hydrothermal treatment (HT) has been favored for the synthesis of lower Si/Al ratio of ZSM-5 containing only one-twentieth TPA^+ ion by which the conventional hydrothermal synthesis of ZSM-5 shows the constraints of realizing this recipe. Under this extreme minimum concentration of TPA^+ ion, neither of the techniques, SAC or conventional hydrothermal treatment, are applicable for extending the purely ZSM-5 synthesis up to a high Si/Al ratio (Si/Al = 100). The resulting solids show the presence of MOR zeolite as phase impurity. The SAC and HT can both be effectively applied to synthesize ZSM-5 with a high as well as a low Si/Al ratio when the TPA^+ ion is only reduced by one-fifth. Simultaneously, hierarchical pore system consisting of micro- and mesopores was obtained during the crystallization of ZSM-5. The presence of these mesopores can be maintained because the zeolite crystal morphology is affected by severe defect sites. The resulting zeolite crystallinity synthesized under one-fifth TPA^+ ion never reaches 100%, similar to the perfect coffin-type crystal despite performing a highly crystalline product. It is summarized that SAC is an appropriate synthesis technique for obtaining low templated ZSM-5, in particular for simultaneously perform a hierarchical pore-type zeolite.

Acknowledgements

The work was supported in part by a TWAS research grant. MR acknowledges the financial support and scholarship from the Indonesian Ministry of Education, Directorate for Higher Education (DIKTI). GTMK acknowledges DIKTI for the scholarship through the PMDSU program. RRM thanks Prof. M. O. Coppens (UCL) and Prof. F. Fajula (U. Montpellier) for a fruitful discussion. We acknowledge Dr. Z. Liu, Dr. T. Wakihara and Prof. T. Okubo for the TEM measurement at The University of Tokyo, Japan.

Appendix A. Supplementary data

Supplementary data related to this article can be found at http://dx.doi.org/10.1016/j.micromeso.2016.04.038.

References

[1] M. Guisnet, J.P. Gilson (Eds.), Zeolite for Cleaner Technologies, Imperial College Press, London, 2002.
[2] W. Vermeiren, J.P. Gilson, Top. Catal. 52 (2009) 1131–1161.
[3] A. Corma, Chem. Rev. 95 (1995) 559–614.
[4] S.M. Csicsery, Pure Appl. Chem. 58 (1986) 841–856.
[5] M.E. Davis, Acc. Chem. Res. 26 (1993) 111–115.
[6] K.B. Yoon, in: J. Cejka, A. Corma, S. Zones (Eds.), Zeolites and Catalysis: Synthesis, Reactions and Applications, vol. 2, Wiley-VCH, Weinham, 2010, pp. 411–447.
[7] V. Sebastian, C. Casado, J. Coronas, in: J. Cejka, A. Corma, S. Zones (Eds.), Zeolites and Catalysis: Synthesis, Reactions and Applications, vol. 2, Wiley-VCH, Weinham, 2010, p. 389.
[8] E.E. McLeary, J.C. Jansen, F. Kapteijn, Microporous Mesoporous Mater. 90 (2006) 198–220.
[9] K. Hoffman, F. Marlow, in: S.M. Auerbach, K.A. Carrado, P.K. Dutta (Eds.), Handbook of Zeolite Science and Technology, Marcel Dekker, Inc., New York, 2003.
[10] K. Pavelic, M. Hadzija, in: S.M. Auerbach, K.A. Carrado, P.K. Dutta (Eds.), Handbook of Zeolite Science and Technology, Marcel Dekker, Inc., New York, 2003.
[11] T.F. Degnan, G.K. Chitnis, P.H. Schipper, Microporous Mesoporous Mater. 35–36 (2000) 245–252.
[12] C.S. Cundy, Chem. Rev. 103 (2003) 663–702.
[13] S.D. Kim, S.H. Noh, K.H. Seong, W.J. Kim, Microporous Mesoporous Mater. 72 (2004) 185–192.
[14] N.Y. Kang, B.S. Song, C.W. Lee, W.C. Choi, K.B. Yoon, Y.K. Park, Microporus Mesoporous Mater. 118 (2009) 361–372.
[15] V.P. Shiralkar, A. Clearfield, Zeolites 9 (1989) 363–370.
[16] M. Otake, Zeolites 14 (1994) 42–52.
[17] R. W. Grose, E. M. Flanigen, US Patent 4 257 885, 1981.
[18] P.A. Jacobs, J.A. Martens, Stud. Surf. Sci. Catal. 33 (1987) 113–146.
[19] B.M. Lowe, J.R.D. Nee, J.L. Casci, Zeolites 14 (1994) 610–619.
[20] N. Ren, Z.J. Yang, X.C. Lv, J. Shi, Y.H. Zhang, Y. Tang, Microporous Mesoporous Mater 131 (2010) 103–114.
[21] Q. Wu, X. Wang, G. Qi, Q. Guom, S. Pan, X. Meng, J. Xu, F. Deng, F. Fan, Z. Feng, C. Li, Maurer, U. Miller, J. Am. Chem. Soc. 136 (2014) 4019–4025.
[22] K. Itabashi, Y. Kamimura, K. Iyoki, A. Shimojima, T. Okubo, J. Am. Chem. Soc. 134 (2012) 11542–11549.
[23] Y. Kamimura, W. Chaikittisilp, K. Itabashi, A. Shimojima, T. Okubo, Chem. Asian J. 5 (2010) 2182–2191.
[24] K. Iyoki, K. Itabashi, T. Okubo, Microporous Mesoporous Mater. 189 (2014) 22–30.
[25] M. Ogura, K. Inoue, T. Yamaguchi, Catal. Today 168 (2011) 118–123.
[26] M. Ogura, Y.W. Zhang, S.P. Elangovan, T. Okubo, Microporous Mesoporous Mater. 101 (2007) 224–230.
[27] M. Matsukata, T. Osaki, M. Ogura, E. Kikuchi, Microporous Mesoporous Mater. 56 (2002) 1–10.
[28] J. Wang, J.C. Groen, W. Yue, W. Zhou, M.O. Coppens, J. Mater. Chem. 18 (2008) 468–474.
[29] J. Wang, J.C. Groen, W. Yue, W. Zhou, M.O. Coppens, Chem. Commun. (2007) 4653–4655.
[30] J. Wang, W. Yue, W. Zhou, M.O. Coppens, Microporous Mesoporous Mater. 120 (2009) 19–28.
[31] M.S. Holm, E. Taarning, K. Egeblad, C.H. Christensen, Catal. Today 168 (2011) 3–16.
[32] M. Moliner, C. Martinez, A. Corma, Angew. Chem. Int. Ed. 54 (2015) 3560–3579.
[33] J. Perez-Ramirez, C.H. Christensen, K. Egeblad, C.H. Christensen, J.C. Groen, Chem. Soc. Rev. 37 (2008) 2530–2542.
[34] M. Choi, K. Na, J. Kim, Y. Sakamoto, O. Terasaki, R. Ryoo, Nature 461 (2009) 246–249.
[35] F.S. Xiao, L. Wang, C. Yin, K. Lin, Y. Di, J. Li, R. Xu, D.S. Su, R. Schloegl, T. Yokoi, T. Tatsumi, Angew. Chem. Int. Ed. 45 (2006) 3090–3093.
[36] R.R. Mukti, H. Hirahara, A. Sugawara, A. Shimojima, T. Okubo, Langmuir 26 (2010) 2731–2735.
[37] M. Choi, H.S. Cho, R. Srivastava, C. Venkatesan, D.H. Choi, R. Ryoo, Nat. Mater. 5 (2006) 718–723.
[38] K. Na, M. Choi, R. Ryoo, Microporous Mesoporous Mater. 166 (2013) 3–19.
[39] G. Majano, L. Delmotte, V. Valtchev, S. Mintova, Chem. Mater. 21 (2009) 4184–4191.
[40] K. Moller, B. Yilmaz, R.M. Jacubinas, U. Mueller, T. Bein, J. Am. Chem. Soc. 133 (2011) 5284–5295.
[41] X. Cheng, J. Mao, X. Lv, T. Hua, X. Cheng, Y. Long, Y. Tang, J. Mater. Chem. A 2 (2014) 1247–1251.
[42] X. Meng, F.S. Xiao, Chem. Rev. 114 (2014) 1521–1543.
[43] M. Thommes, B. Smarsly, M. Groenewolt, P.I. Ravikovitch, A.V. Neimark, Langmuir 22 (2006) 756–764.
[44] Y. Tao, H. Kanoh, K. Kaneko, Adv. Mater. 17 (2005) 2789–2792.
[45] K.K. Unger, J. Rouquerol, K.S.W. Sing, H. Kral, Characterization of Porous Solids, vol. 39, Elsevier, Amsterdam, 1988, p. 101.
[46] M. Kruk, M. Jaroniek, Chem. Mater. 12 (2000) 222–230.
[47] J. Wang, J.C. Groen, M.O. Coppens, J. Phys. Chem. C 112 (2008) 19336–19345.